

Observation of the solid-state photo-CIDNP effect in entire cells of cyanobacteria *Synechocystis*

Geertje J. Janssen · Eugenio Daviso ·
Martin van Son · Huub J. M. de Groot ·
A. Alia · Jörg Matysik

Received: 9 July 2009 / Accepted: 25 November 2009 / Published online: 22 January 2010
© The Author(s) 2010. This article is published with open access at Springerlink.com

Abstract Cyanobacteria are widely used as model organism of oxygenic photosynthesis due to being the simplest photosynthetic organisms containing both photosystem I and II (PSI and PSII). Photochemically induced dynamic nuclear polarization (photo-CIDNP) ^{13}C magic-angle spinning (MAS) NMR is a powerful tool in understanding the photosynthesis machinery down to atomic level. Combined with selective isotope enrichment this technique has now opened the door to study primary charge separation in whole living cells. Here, we present the first photo-CIDNP observed in whole cells of the cyanobacterium *Synechocystis*.

Keywords Plant photosystems · Photo-CIDNP · Electron transfer · Solid-state NMR

Abbreviations

ALA	δ -Aminolevulinic acid
Chl	Chlorophyll
DD	Differential decay
DR	Differential relaxation
Hf	Hyperfine
LC-MS	Liquid chromatography-mass spectrometry
MAS	Magic angle spinning
photo-CIDNP	Photochemically induced dynamic nuclear polarization
PBG	Pyrrole porphobilinogen
PS1 PS2	Photosystems I, II
TSM	Three-spin mixing

Introduction

Natural photosynthesis, occurring in plants, algae and several types of bacteria, is initiated by highly efficient light-induced electron transfer occurring in reaction center (RC) proteins having a quantum yield close to unity. It has been proposed that this remarkable efficiency is related to the occurrence of correlated radical pairs (Thurnauer and Norris 1980) and the solid-state photo-CIDNP effect (Matysik et al. 2009).

Photochemical-induced dynamic nuclear polarization (photo-CIDNP) is a well-known phenomenon in liquid NMR (for review: Hore and Broadhurst 1993; Roth 1996; Goetz 1997), discovered in 1967 (Bargon and Fischer 1967; Bargon et al. 1967; Ward and Lawler 1967; Cocivera 1968) which has been explained by the radical pair mechanism (RPM) (Closs and Closs 1969; Kaptein and Oosterhoff 1969). In 1994, Zysmilich and McDermott observed for the first time this new type of photo-CIDNP in frozen and quinone-blocked RCs of purple bacteria of *Rhodobacter (Rb.) sphaeroides* R26 by ^{15}N magic-angle spinning NMR (Zysmilich and McDermott 1994). Meanwhile, the exact spin-chemical mechanism of the solid-state photo-CIDNP effect (for reviews: Jeschke and Matysik 2003; Daviso et al. 2008) in this system is understood (Daviso et al. 2009a, b). Initially, the spin-correlated radical pair is formed in a pure singlet state (Fig. 1) and it is, therefore, highly electron polarized. This electron polarization can be observed by EPR as photo-CIDEP. Three mechanisms occur to build up photo-CIDNP under continuous illumination, which run in parallel. In all mechanisms, the break of the balance of the opposite nuclear spin populations in the two decay branches of the radical pair states leads to *net* steady-state nuclear polarization, which is detected in the NMR experiment: (i) Electron–electron–

G. J. Janssen · E. Daviso · M. van Son ·
H. J. M. de Groot · A. Alia (✉) · J. Matysik
Leiden Institute of Chemistry, Leiden University, Einsteinweg
55, P.O. Box 9502, 2300 RA Leiden, The Netherlands
e-mail: a.alia@chem.leidenuniv.nl

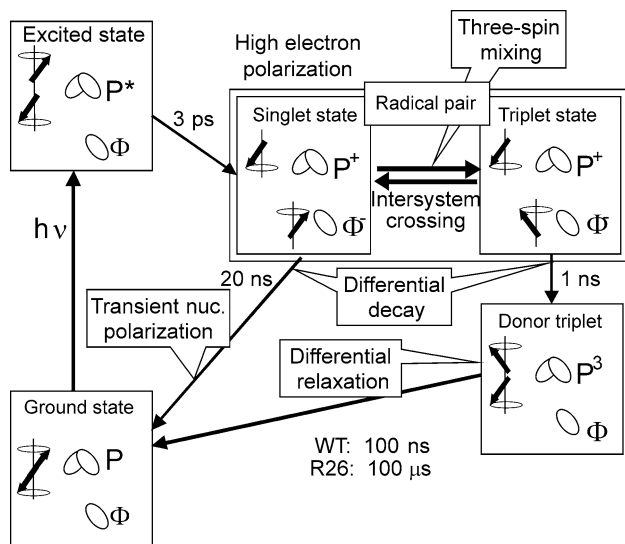


Fig. 1 The mechanisms of photo-CIDNP production in natural RCs of *Rb. sphaeroides* WT and R26 as established for high-field conditions. From the photochemically excited donor, P^* , an electron is transferred to the primary acceptor Φ , a bacteriopheophytin. The radical pair ($P^+\Phi^-$) is initially in a pure singlet state and thus highly electron polarized. Due to hyperfine interaction, the radical pair is oscillating between a singlet and a T_0 triplet state. During intersystem crossing (ISC), electron polarization is transferred to nuclei by three-spin mixing (TSM). Back-ET from the singlet state of the radical pair leads to the electronic ground-state. Back-ET from the triplet state of the radical pair leads to the donor triplet (3P) state. In the differential decay (DD) mechanism, *net* photo-CIDNP is produced by different contributions of the two spin states of the spin-correlated radical pair to the spin evolution. In RCs having a long lifetime of the donor triplet, 3P , as in R26, the differential relaxation (DR) mechanism occurs since nuclear spin relaxation is significant on the triplet branch, causing incomplete cancellation of nuclear polarization of both branches

nuclear three-spin mixing (TSM) breaks the balance of the two radical-pair decay channels by spin evolution within the correlated radical pair state depending on the signs of the electron–electron and of the electron nuclear interactions (Jeschke 1997, 1998). This process occurs during intersystem crossing (ISC) in solids. The flow of polarization from electrons to nuclei is driven by the pseudosecular (off-diagonal) part B of the hyperfine (hf) interaction. (ii) In the differential decay (DD) mechanism (Polenova and McDermott 1999), the symmetry between the two decay channels is broken by the different lifetimes of the states of the correlated radical pair. This means that in the two radical pair spin states different fractions of polarization flow from the electrons to the nuclei. The result is an additional imbalance between the fractions of nuclei in spin-up and spin-down states in the two decay channels. (iii) In addition to the two polarization transfer mechanisms TSM and DD, in samples as R26-RCs of *Rb. sphaeroides* having a long lifetime of the triplet donor (3P), a third mechanism may occur that creates nuclear polarization: in the differential relaxation (DR)

mechanism, the breaking of antisymmetry of the polarization in the singlet and triplet branch occurs in a non-coherent way. The enhanced relaxation of nuclear spins in the proximity of the high-spin donor partially cancels the nuclear polarization in the donor cofactor. Hence, when the 3P lifetime is comparable to or exceeds the paramagnetically enhanced longitudinal relaxation time, net polarization occurs due to partial extinction of nuclear polarization of the triplet state of the radical pair (Goldstein and Boxer 1987; McDermott et al. 1998).

The number of RCs have proven to show the solid-state photo-CIDNP effect is growing. The list contains systems from various bacteria as well as from plants as bacterial RCs of *Rb. sphaeroides* WT (Prakash et al. 2005; Daviso et al. 2009b) and R26 (Prakash et al. 2006), *Rhodospseudomonas acidophila* (Diller et al. 2008), *Chlorobium tepidum* (Roy et al. 2007) and *Heliobacillus mobilis* (Roy et al. 2008) as well as in RCs of plant photosystems I and II (Matysik et al. 2000; Alia et al. 2004; Diller et al. 2007). It appears that the occurrence of the solid-state photo-CIDNP effect is an intrinsic property of photosynthetic RCs (Roy et al. 2008; Matysik et al. 2009) despite the window of occurrence of this effect is rather limited by kinetic and magnetic parameters (Jeschke and Matysik 2003; Daviso et al. 2008). Initially, photo-CIDNP MAS NMR experiments were performed on isolated RCs. Later, it became evident that the strong enhancement effect also allows for investigations directly on cells (Prakash et al. 2006) or photosynthetic membranes (Roy et al. 2008).

In the growing list of natural RCs proven to show the solid-state photo-CIDNP effect, RCs of cyanobacteria (blue algae) remained an open question. Cyanobacteria are model microorganisms for the study of plant photosynthesis having a photosynthetic apparatus very similar to the one found in plants. In particular, cyanobacterium *Synechocystis* is of interest, which can grow both autotrophically or heterotrophically in the absence of light and is easily transformed by exogenous DNA. Here, we present photo-CIDNP ${}^{13}C$ MAS NMR data obtained directly from whole cells of cyanobacterium *Synechocystis*.

Materials and methods

Strains and culture conditions

Wild-type cyanobacterium *Synechocystis* sp. PCC 6803 strain was kindly provided by A.H.M. de Wit of the Biophysics group of Leiden University. Cultures were grown at 25°C in standard BG-11 medium (Allen 1968) and illuminated by fluorescent white lamps giving a total intensity of 50 $\mu E m^{-2} s^{-1}$. Cultures were bubbled with 5% CO_2 -enriched air to promote growth. Selective isotope

enrichment of chlorophyll (Chl) in *Synechocystis* was done by growing the cyanobacterium in BG-11 medium supplemented with [4-¹³C]- δ -aminolevulinic acid ([4-¹³C]-ALA) purchased from Cambridge Isotope Laboratories (99% ¹³C-enriched) to a final concentration of 53 mM.

Determination of the ¹³C incorporation

Chl *a* was purified from cells grown in [4-¹³C]-ALA-supplemented BG-11 medium (labeled sample) and from unlabeled cells (reference sample), according to the following procedure: cells were harvested by centrifugation for 10 min at 13.2 krpm. The cell pellet was resuspended in 1 ml methanol, shaken and centrifuged for 5 min at 2 krpm after which the green supernatant was collected. This procedure was repeated until the pellet showed a white-bluish color. The solvent was evaporated under nitrogen (low light conditions were kept for the entire purification procedure) and the obtained pigments resuspended in 2,500 μ l running solution, 70:30 (v/v) petroleum ether/acetone. This was loaded on a column filled with silica gel (particle size 40–63 μ m, pore diameter \sim 60 Å) and washed with running solution. Fractions containing pure Chl *a* were identified using a Shimadzu UV–visible spectrophotometer, combined, dried under nitrogen and stored at -20°C .

LC-MS

Mass spectra were measured on a LTQ–FT hybrid mass spectrometer (Thermo Fisher Waltham, MA, USA). Spectra were measured in ESI mode, with a source temperature of 200°C, source voltage of 3.8 kV and tube lens voltage 150 V. Chl *a* was dissolved in 90% EtOH and 10% 10 mM ammonium acetate to a final concentration of \sim 1 mg/ml. The sample was infused with a flow rate of 10 μ l/min.

MAS NMR sample preparation

Selectively isotope-enriched *Synechocystis* cells were harvested by centrifugation and washed once with standard BG-11 medium. The pellet was resuspended in a 100 μ l of standard BG-11 under low light conditions. The sample was bubbled shortly with nitrogen to remove oxygen and quinone reduced by adding sodium dithionite to a final concentration of 100 mM under oxygen free and near dark conditions. After 30 min of incubation in the dark at room temperature, the sample was loaded into an optical transparent 4-mm sapphire MAS rotor under oxygen free conditions. The sample was inserted into the NMR spectrometer right away. The isolated samples of PS1 and PS2 from spinach (*Spinacia oleracea*) at natural abundance have been prepared following the procedures described in Matsyik et al. (2000) and Alia et al. (2004).

Photo-CIDNP MAS NMR experiments

¹³C-MAS NMR experiments were performed on a DMX-200 NMR spectrometer (Bruker Biospin GmbH, Karlsruhe, Germany). All spectra have been obtained at a sample temperature of 235 K and a spinning speed of 8 kHz. The spectra were collected with a spin echo pulse sequence with the CYCLOPS phase cycle of ($\pi/2$) pulse under TPPM carbon-proton decoupling. Photo-CIDNP MAS NMR spectra have been obtained under continuous illumination with a 1,000-W xenon arc lamp.

Results and discussion

Determination of the ¹³C label incorporation

The biosynthetic route from [4-¹³C]-ALA to Chl *a* is depicted in Fig. 2. Two molecules of [4-¹³C]-ALA are asymmetrically condensed to form the pyrrole porphobilinogen (PBG). Four molecules of PBG tetramerize, and prior to macrocycle ring closure, the last pyrrole ring is inverted via a spiro-intermediate (Schulten et al. 2002). Upon incorporation of [4-¹³C]-ALA, a maximum of 8 ¹³C can be pair wise incorporated into each Chl *a* molecule, resulting into the specific labeling pattern shown in Fig. 2 with ¹³C isotopes incorporated on position C-1/C-3, C-6/C-8, C-11/C-13, and C-17/C-19. The level of [4-¹³C]-ALA incorporation was determined quantitatively by LC-MS analysis. Chl *a* pigments were extracted from *Synechocystis* cells grown in [4-¹³C]-ALA supplemented BG-11 (labelled sample), and normal BG-11 medium (reference sample). Figure 3 shows the LC-MS spectra observed in the region of $m/z = 893.5$ ($[\text{M}]^+$; $\text{C}_{55}\text{H}_{72}\text{O}_5\text{N}_4\text{Mg}$) from the reference (A) and the labelled sample (B). The total level of incorporation (P_{tot}) was determined through an iterative procedure as described earlier in (Schulten et al. 2002) making use of a weighted sum according to the formula:

$$P_{\text{tot}} = \sum_{n=0}^8 \frac{n}{8} \times P_n \quad (1)$$

where n stands for the number of labels present in an isotopomer and P_0 is the corresponding fraction of unlabelled Chl *a* estimated from the isotopic labeling pattern detected from the reference sample (Fig. 3a). Analysis of the isotopic patterns depicted in Fig. 3 reveal P_1 – P_6 within the same Chl *a* molecule ranging from 1 to 6% and P_7 – P_8 equal to 0. The weighted sum of these separate contributions according to Eq. 1 corresponds to a total incorporation of the 8 ¹³C isotope labels with $P_{\text{tot}} = 30 \pm 5\%$.

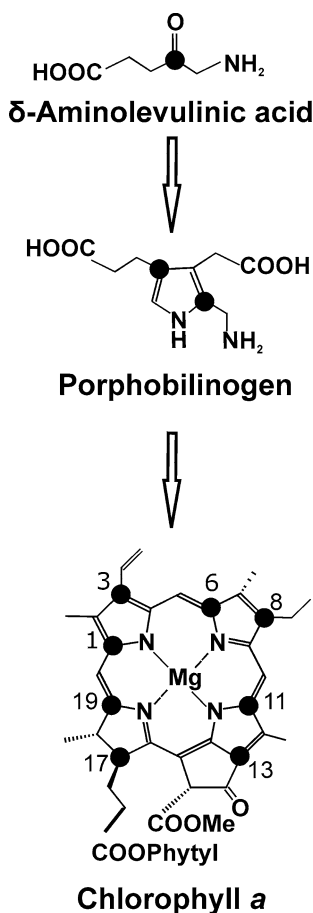


Fig. 2 Incorporation of [4- ^{13}C]-ALA into Chl *a*, black dots indicate ^{13}C isotopes

Occurrence of the solid-state photo-CIDNP effect in *Synechocystis*

Spectrum A in Fig. 4 shows a ^{13}C MAS NMR spectrum of *Synechocystis* cells containing [4- ^{13}C]-ALA-labelled Chl *a* and Phe *a* cofactors obtained in the dark. The spectrum shows, as expected, signals in the aliphatic region between 0 and 50 ppm, in the aromatic region as well as in the region of the amide carbonyls. Probably, the aromatic carbons appear due to the isotope labelling. Upon illumination with continuous white light (Spectrum 4B), additional signals occur between 170 and 120 ppm. All light-induced signals in that region are emissive (negative). It is also possible that light-induced signals appear in the aliphatic region between 50 and 80 ppm, although dark signals and the high noise level may interfere.

Spectrum C in Fig. 4 shows a ^{13}C MAS NMR spectrum of another preparation of *Synechocystis* cells without isotope label incorporation obtained under continuous illumination. Under these conditions, it is difficult to identify light-induced signals, although there may be some weekly emissive signal appearing at about 150 ppm.

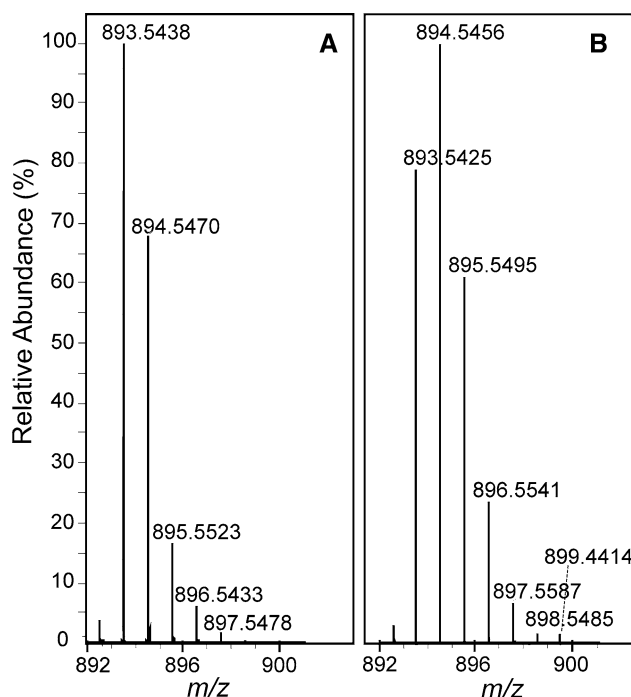


Fig. 3 Patterns observed with LC-MS spectroscopy around $m/z = 893$ from natural abundance Chl *a* (a) and $^{13}\text{C}_{0-8}$ Chl *a* (b)

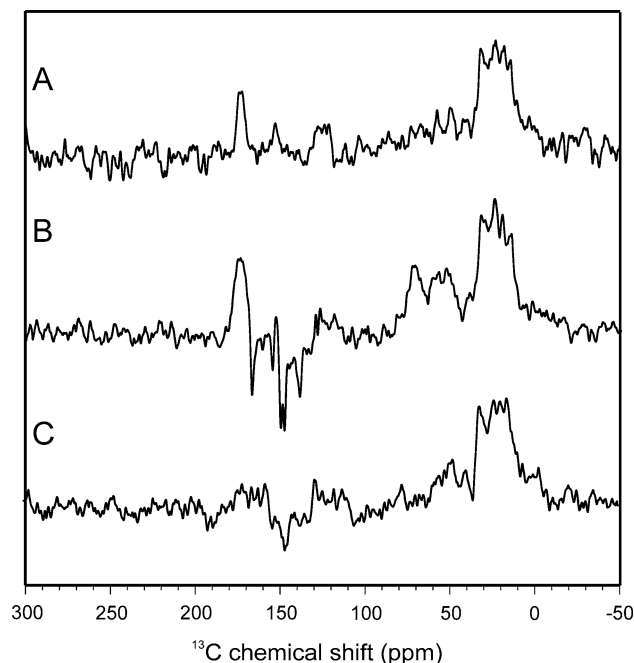


Fig. 4 ^{13}C MAS NMR spectra of fresh *Synechocystis* cells obtained under dark conditions (a), and under continuous illumination with white light (b) of cells grown in [4- ^{13}C]-ALA-supplemented BG-11 medium. Spectrum C shows data obtained under continuous illumination of fresh *Synechocystis* cells grown in normal BG-11 medium. All spectra have been obtained at a temperature of 235 K, a magnetic field of 4.7 Tesla and a MAS frequency of 8 kHz

Until now, only in one other single cell system, the purple bacterium *Rb. sphaeroides* R26 (Prakash et al. 2006) has the observation of the solid-state photo-CIDNP effect been reported. In that system, only one type of RC is present and no isotope labelling was necessary. Here, we show that the solid-state photo-CIDNP effect can also be observed in intact cyanobacterial cells containing both PS1 and PS2. In order to recognize light-induced signals in *Synechocystis*, however, specific isotope labelling was necessary. Assuming that the solid-state photo-CIDNP effect would be of similar strength as in RCs of *Rb. sphaeroides* R26, the necessity to use labels suggest that the intensity of the light-induced signals is about a factor 30 weaker. The origin of this lack of intensity may be (i) insufficient reduction of the acceptor site, (ii) lower concentration of the photosystems caused by the presence of other cellular units, or (iii) the destructive interference of the signals from PS1 and PS2.

Assignment of light-induced signals

Spectrum A in Fig. 5 shows a zoom of the aromatic region of Spectrum 4B. The light-induced signals visualized by the dashed lines originate from the [4- ^{13}C]-ALA-labelled Chl *a* and Phe *a* cofactors. Table 1 shows the chemical shifts of the observed signals and of literature values of light-induced signals from Chl *a* aggregates and isolated PS1 and D1D2 particles (Boender et al. 1995; Alia et al. 2004; Diller et al. 2005). With the possible exception of the absorptive feature at 153.4 ppm (see below), all light-induced signals are of emissive nature.

As suggested by Table 1, most of the light-induced signals observed in *Synechocystis* cells appear at frequencies matching very well with those observed in isolated photosystems of spinach. For example, the signals at 166.9, 154.8, 147.6, 144.2, and 138.6 ppm are observed in isolated PS1 at very similar frequencies. This similarity suggests that photosystems are highly conserved even between different families. We also conclude that the isolation of the photosystems from plants did not significantly affect the electronic properties of the photochemical machinery.

Spectra B and C in Fig. 5 show ^{13}C photo-CIDNP MAS NMR data obtained from isolated PS1 and PS2, respectively, from spinach at natural abundance. The spectrum of PS1 is entirely emissive in the aromatic region (Spectrum 5B). In contrast, the spectrum of PS2 shows in the region from 180 to 130 ppm only absorptive signals (Spectrum 5C). Therefore, it is reasonable to assume that all emissive signals in Spectrum 5A arise from PS1. Three possible reasons may explain the absence of PS2 resonances: (i) The PS1/PS2 ratio in *Synechocystis* is known to be in strong favor of PS1 with PS2 being up to nine times less abundant (Rögner et al. 1990), (ii) PS2 proteins may degrade under experimental conditions with strong illumination (iii) The

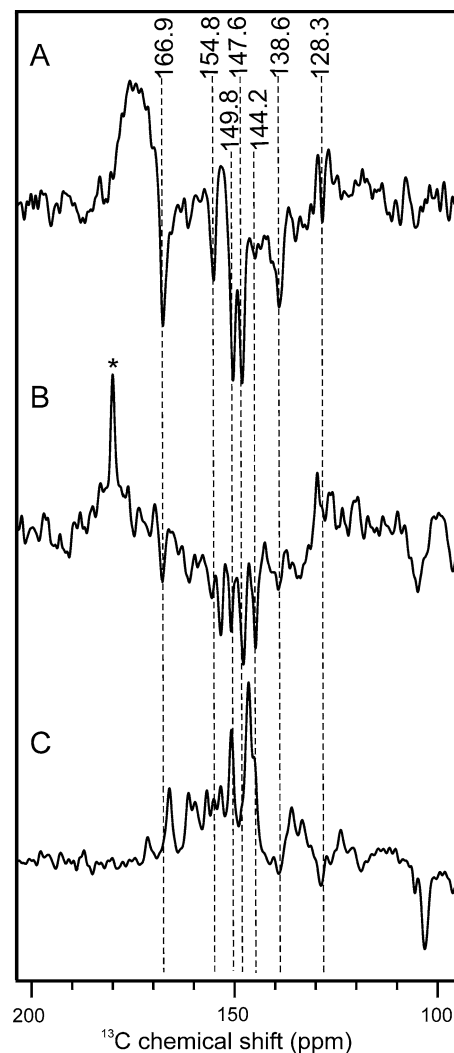


Fig. 5 ^{13}C MAS NMR spectra of fresh [4- ^{13}C]-ALA-labelled *Synechocystis* cells (a), and from isolated PS1 (b) and PS2 (c) particles from spinach at natural abundance. Spectrum A depicts a zoom of the aromatic region of Spectrum 4A. Assigned centerbands are visualized by dashed lines. In Spectrum B the absorptive signal from the sucrose buffer is marked by an asterisk. All three spectra have been obtained under continuous illumination by white light at a temperature of 235 K, magnetic field of 4.7 Tesla and MAS frequency of 8 kHz

chemical shifts of the signals from PS1 and PS2 are very similar at the isotope-labelled positions (Table 1), therefore, absorptive PS2 signals may be cancelled by dominating emissive PS1 signals. Hence, the emissive photo-CIDNP signals in the aromatic region can be assigned to the specifically isotope-labelled carbons C-1, C-3, C-6, C-8, C-11, C-13, and C-19 (Fig. 2) of PS1.

There are, however, two absorptive signals which may be light-induced, too. These are the signals at ~ 170 and 153.4 ppm. Indeed, comparison with Spectrum 5C suggests that at these positions positive signals occur from PS2 without being completely cancelled by emissive PS1 signals.

Table 1 ^{13}C chemical shifts of the photo-CIDNP signals obtained at 4.7 T in comparison to literature

Chemical shifts				
Chl <i>a</i> $\sigma_{\text{ss}}^{\text{a}}$	Assignment atom	PS1 σ^{b}	PS2 σ^{c}	PS1 + PS2 σ^{d}
170.0	19	167.1 E	166.8 A	166.9 E
162.0	14	160.4 E	162.2 A	
155.9	1	154.8 E	156.0 A	154.8 E
154.4	6		154.3 A	149.8 E
154.0	16	152.6 E	151.6 A	
150.7	4	149.9 E	149.2 A	
147.2	11	147.2 E	147.7 A	147.6 E
147.2	9			
146.2	8	144.2 E	146.0 A	144.2 E
138.0	3	138.6 E	137.4 A	138.6 E
136.1	2	~136 E	136.0 A	
134.0	12		133.9 A	
133.4	7	~132 E	~132.0 A	
126.2	13			128.3 E
108.2	10	105.4 E	106.9 E	~104.5 E
102.8	15		104.7 E	
98.1	5		97.9 E	
93.3	20		92.2 E	
51.4	17			53.9

^a Boender (1995), data obtained from solid aggregates of Chl *a*.

^b Alia et al. (2004), data obtained from isolated PS1 particles from spinach. ^c Diller et al. (2005), data obtained from DID2 particles of spinach. ^d This work, data obtained from living *Synechocystis* whole cells containing both PS1 and PS2. Abbreviations: σ = chemical shift, *A* absorptive signal, *E* emissive signal

In addition, two broad absorptive humps occur with maxima around 70 and 50 ppm (Spectrum 4B). Signals of C-17 are indeed expected in this region. Since for continuous illumination experiments of selectively labelled RCs, labelled aliphatic carbons may gain intensity indirectly by spin diffusion from the labelled aromatic carbons nearby (Matysik et al. 2001), the origin of the enhancement is not obvious. A possible explanation may be that these positive light-induced signals indeed originate from PS2, while the light-induced signals in the aromatic region originate from PS1. In that case, the PS2 signal would be suppressed in the aromatic region but would dominate the aliphatic region due to different relaxation properties that would imply that the above-discussed weakness of the signals is caused by an almost complete destructive interference of PS1 and PS2 signals. Investigation on systems having a strongly modified ratio between PS1 and PS2 may provide this insight.

Activity of sample upon storage

Photo-CIDNP signals have been observed exclusively in samples prepared from *freshly* harvested cells. Samples

prepared from previously frozen [4- ^{13}C]-ALA-labelled cells, which were otherwise treated identically, did not show the solid-state photo-CIDNP effect (not shown). Also, samples prepared from freshly harvested cells lost about 70% of the photo-CIDNP intensity after being re-investigated after several weeks of storage at -20°C . In contrast, previously used samples of isolated PS1 or DID2-PS2 particles of spinach (Alia et al. 2004; Diller et al. 2005) did not show a significant loss of activity after storage at -20°C for up to several years. It appears that isolation increases stability upon storage and that the occurrence of the solid-state photo-CIDNP effect in whole cells requires samples at highly natural conditions.

Light-induced changes in the sample

Using a freshly harvested sample, signals started to appear after 12 h of measurement. In contrast, in a sample already exposed to 50 h of white light, photo-CIDNP signals arose after 4 h (data not shown).

Figure 6 shows the aromatic region of two ^{13}C MAS NMR spectra of fresh [4- ^{13}C]-ALA-labeled *Synechocystis* cells obtained under continuous illumination with white light from 0 to 25 h (solid line) and 50 to 75 h (dashed line). It seems that signals typical for PS2 (Spectrum 5C) diminish upon extended illumination. In particular, the positive features at 170 and 153.4 ppm as well as the emissive signal at 104.5 ppm are significantly weakened in the second data set.

A possible explanation could rely on the fact that PS1 is, compared to PS2, known to be very difficult to reduce (Feldman et al. 2007) and its reduction might be ongoing during the measurement at 235 K. This is in agreement with the observation that upon decreasing the incubation time after reduction with sodium dithionite from 30 to 10 min, the emissive signals assigned to PS1 are weakened significantly, while the absorptive feature at 153.4 ppm is strongly enhanced (data not shown). It may be that the absorptive resonances of more efficiently reduced PS2 initially cancel the build up of emissive PS1 signals. Since PS1 is much more robust than PS2 (Mattoo et al. 1984) after several hours of illumination PS2 may be degraded, allowing for a faster build up of PS1 signals. Indeed, it seems that typical markers of the PS2 spectrum decay while PS1 signals remain. For example, the signal at ~ 104.5 ppm diminishes upon prolonged illumination.

Summary and outlook

The solid-state photo-CIDNP effect appears to be highly conserved in photosynthetic systems as proposed earlier (Matysik et al. 2009). In this study, the occurrence of the

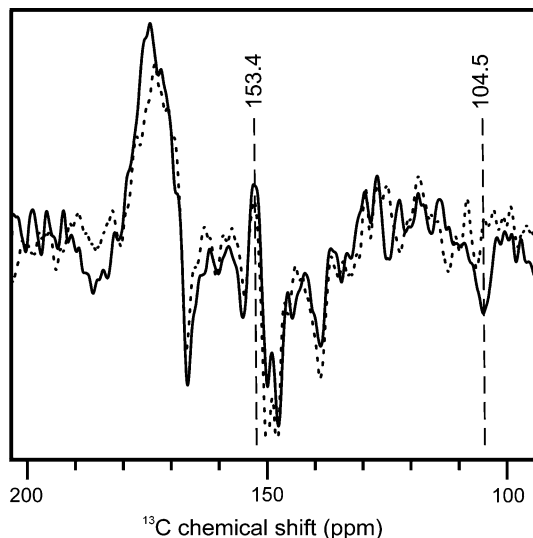


Fig. 6 ^{13}C MAS NMR spectra of fresh $[4\text{-}^{13}\text{C}]$ -ALA labelled *Synechocystis* cells obtained under continuous illumination with white light from 0 to 25 h (solid) and 50 to 75 h (dashed). 104.5 and 153.4 ppm centerbands are visualized by dashed lines

solid-state photo-CIDNP effect has been demonstrated in cyanobacteria. In addition, the photo-CIDNP features of PS1 and PS2 appear to be very similar in plant and cyanobacterial systems, suggesting remarkable conservation of the electronic properties of their photochemical machineries. The occurrence of the effect also in cyanobacterial photosystems directly in cells implies that photo-CIDNP MAS NMR studies on oxygenic photosystems are not any longer limited to isolated plant photosystems.

Acknowledgments The authors thank B. Bode, G. Jeschke, K.B. Sai Sankar Gupta, J. Lugtenburg, and S. Tamarath-Surendran and R. Vreeken for stimulating discussions. A. H. M. de Wit for providing the *Synechocystis* strain. G. Spijksma for recording the LC-MS spectra. The help of F. Lefeber, K. B. Sai Sankar Gupta, A. Oudshoorn, W. P. van Oordt, W. Vermaas, and K. Erkelens is gratefully acknowledged. This study has been financially supported by the Netherlands Organization for Scientific Research (NWO) through a Vidi grant (700.53.423) to J. Matysik.

Open Access This article is distributed under the terms of the Creative Commons Attribution Noncommercial License which permits any noncommercial use, distribution, and reproduction in any medium, provided the original author(s) and source are credited.

References

- Alia, Roy E, Gast P et al (2004) Photochemically induced dynamic nuclear polarization in photosystem I of plants observed by C-13 magic-angle spinning NMR. *J Am Chem Soc* 126:12819–12826
- Allen MM (1968) Simple conditions for growth of unicellular blue-green algae on plates. *J Phycol* 4:1–4
- Bargon J, Fischer H (1967) Kernresonanz-Emissionslinien während rascher Radikalreaktionen. 2. Chemisch induzierte dynamische Kernpolarisation. *Z Naturforsch A* 22:1556–1562
- Bargon J, Fischer H, Johnson U (1967) Kernresonanz-Emissionslinien während rascher Radikalreaktionen I. Aufnahmeverfahren und Beispiele. *Z Naturforsch A* 22:1551–1555
- Boender GJ, Raap J, Prytulla S et al (1995) MAS NMR structure refinement of uniformly C-13 enriched chlorophyll-*a* water aggregates with 2D dipolar correlation spectroscopy. *Chem Phys Lett* 237:502–508
- Closs GL, Closs LE (1969) Induced dynamic nuclear spin polarization in reactions of photochemically and thermally generated triplet diphenylmethylene. *J Am Chem Soc* 91:4549–4550
- Cocivera M (1968) Optically induced Overhauser effect in solution. Nuclear magnetic resonance emission. *J Am Chem Soc* 90:3261–3263
- Daviso E, Jeschke G, Matysik J (2008) Photo CIDNP MAS NMR. In: Aartsma TJ, Matysik J (eds) *Biophysical techniques in photosynthesis II*. Springer, Dordrecht
- Daviso E, Alia A, Prakash S et al (2009a) Electron-nuclear spin dynamics in a bacterial photosynthetic reaction center. *J Phys Chem C* 113:10269–10278
- Daviso E, Prakash S, Alia A, et al (2009b) The electronic structure of the primary electron donor of purple bacteria at atomic resolution as observed by photo-CIDNP ^{13}C MAS NMR. *Proc Natl Acad Sci USA*. <http://www.pnas.org/content/early/2009/12/10/0908608106.abstract>
- Diller A, Alia A, Roy E et al (2005) Photo-CIDNP solid-state NMR on photosystems I and II: what makes P680 special? *Photosynth Res* 84:303–308
- Diller A, Roy E, Gast P et al (2007) N-15 photochemically induced dynamic nuclear polarization magic-angle spinning NMR analysis of the electron donor of photosystem II. *Proc Natl Acad Sci USA* 104:12767–12771
- Diller A, Gast P, Jeschke G, et al (2008) ^{13}C photo-CIDNP MAS NMR on the LH1-RC complex of *Rhodospseudomonas acidophila*. In: Allen J, Gantt E, Golbeck J, Osmond B (eds) *Energy from the sun*. Springer, Dordrecht
- Feldman KS, Hester DK, Golbeck JH (2007) A relationship between amide hydrogen bond strength and quinone reduction potential: Implications for photosystem I and bacterial reaction center quinone function. *Bioorg Med Chem Lett* 17:4891–4894
- Goez M (1997) Photochemically induced dynamic nuclear polarization. In: Neckers DC, Volmann DH, von Bünau G (eds) *Advance in photochemistry*. Wiley, New York
- Goldstein RA, Boxer SG (1987) Effects of nuclear-spin polarization on reaction dynamics in photosynthetic bacterial reaction centers. *Biophys J* 51:937–946
- Hore PJ, Broadhurst RW (1993) Photo-CIDNP of biopolymers. *Prog Nucl Magn Reson Spectrosc* 25:345–402
- Jeschke G (1997) Electron-electron-nuclear three-spin mixing in spin-correlated radical pairs. *J Chem Phys* 106:10072–10086
- Jeschke G (1998) A new mechanism for chemically induced dynamic nuclear polarization in the solid state. *J Am Chem Soc* 120:4425–4429
- Jeschke G, Matysik J (2003) A reassessment of the origin of photochemically induced dynamic nuclear polarization effects in solids. *Chem Phys* 294:239–255
- Kaptein R, Oosterhoff JL (1969) Chemically induced dynamic nuclear polarization: relation with anomalous ESR spectra. *Chem Phys Lett* 4:195
- Mattoo AK, Hoffmanfalk H, Marder JB et al (1984) Regulation of protein-metabolism—coupling of photosynthetic electron-transport to in vivo degradation of the rapidly metabolized 32-kilodalton protein of the chloroplast membranes. *Proc Natl Acad Sci USA* 81:1380–1384
- Matysik J, Alia, Gast P et al (2000) Photochemically induced nuclear spin polarization in reaction centers of photosystem II observed by C-13 solid-state NMR reveals a strongly asymmetric

- electronic structure of the P-680⁺ primary donor chlorophyll. Proc Natl Acad Sci USA 97:9865–9870
- Matysik J, Schulten E, Alia et al (2001) Photo-CIDNP C-13 magic angle spinning NMR on bacterial reaction centres: exploring the electronic structure of the special pair and its surroundings. Biol Chem 382:1271–1276
- Matysik J, Diller A, Roy E et al (2009) The solid-state photo-CIDNP effect. Photosynth Res. online, doi: [10.1007/s11120-009-9403-9](https://doi.org/10.1007/s11120-009-9403-9)
- McDermott A, Zysmilich MG, Polenova T (1998) Solid state NMR studies of photoinduced polarization in photosynthetic reaction centers: mechanism and simulations. Solid State Nucl Magn Reson 11:21–47
- Polenova T, McDermott AE (1999) A coherent mixing mechanism explains the photoinduced nuclear polarization in photosynthetic reaction centers. J Phys Chem B 103:535–548
- Prakash S, Alia, Gast P et al (2005) Magnetic field dependence of photo-CIDNP MAS NMR on photosynthetic reaction centers of *Rhodobacter sphaeroides* WT. J Am Chem Soc 127:14290–14298
- Prakash S, Alia, Gast P et al (2006) Photo-CIDNP MAS NMR in intact cells of *Rhodobacter sphaeroides* R26: molecular and atomic resolution at nanomolar concentration. J Am Chem Soc 128:12794–12799
- Rögner M, Nixon PJ, Diner BA (1990) Purification and characterization of photosystem-I and photosystem-II core complexes from wild-type and phycocyanin-deficient strains of the cyanobacterium *Synechocystis* PCC-6803. J Biol Chem 265:6189–6196
- Roth HD (1996) Dependence of the yield of a radical-pair reaction in the solid-state on orientation in a magnetic-field. In: Grant DM, Harris RK (eds) Encyclopedia of nuclear magnetic resonance. Wiley, Chichester
- Roy E, Alia, Gast P et al (2007) Photochemically induced dynamic nuclear polarization in the reaction center of the green sulphur bacterium *Chlorobium tepidum* observed by C-13 MAS NMR. Biochim Biophys Acta 1767:610–615
- Roy E, Rohmer T, Gast P et al (2008) Characterization of the primary radical pair in reaction centers of *Heliobacillus mobilis* by ¹³C photo-CIDNP MAS NMR. Biochemistry 47:4629–4635
- Schulten EAM, Matysik J, Alia et al (2002) C-13 MAS NMR and photo-CIDNP reveal a pronounced asymmetry in the electronic ground state of the special pair of *Rhodobacter sphaeroides* reaction centers. Biochemistry 41:8708–8717
- Thurnauer MC, Norris JR (1980) An electron-spin echo phase-shift observed in photosynthetic algae—possible evidence for dynamic radical pair interactions. Chem Phys Lett 76:557–561
- Ward HR, Lawler RG (1967) Nuclear magnetic resonance emission and enhanced absorption in rapid organometallic reactions. J Am Chem Soc 89:5518–5519
- Zysmilich MG, McDermott A (1994) Photochemically induced dynamic nuclear-polarization in the solid-state N-15 spectra of reaction centers from photosynthetic bacteria *Rhodobacter sphaeroides* R26. J Am Chem Soc 116:8362–8363